

# Lawrence Berkeley National Laboratory

## LBL Publications

### Title

THE SURFACE STRUCTURES OF VAPOR-GROWN ICE and NAPHTHALENE CRYSTALS STUDIED BY LOW-ENERGY ELECTRON DIFFRACTION

### Permalink

<https://escholarship.org/uc/item/5db891rq>

### Author

Firment, L.E.

### Publication Date

1975-09-01

Submitted to Surface Science

RECEIVED  
SEP 11 1975  
A 1-105  
LAWRENCE BERKELEY  
LABORATORY

LBL-4154  
Preprint c. |

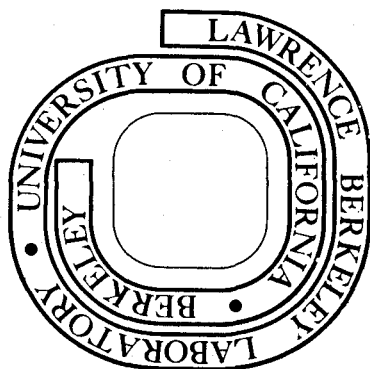
THE SURFACE STRUCTURES OF VAPOR-GROWN ICE AND  
NAPHTHALENE CRYSTALS STUDIED BY LOW-ENERGY  
ELECTRON DIFFRACTION

L. E. Firment and G. A. Somorjai

September 1975

Prepared for the U. S. Energy Research and  
Development Administration under Contract W-7405-ENG-48

**For Reference**  
Not to be taken from this room



LBL-4154  
c. |

## **DISCLAIMER**

This document was prepared as an account of work sponsored by the United States Government. While this document is believed to contain correct information, neither the United States Government nor any agency thereof, nor the Regents of the University of California, nor any of their employees, makes any warranty, express or implied, or assumes any legal responsibility for the accuracy, completeness, or usefulness of any information, apparatus, product, or process disclosed, or represents that its use would not infringe privately owned rights. Reference herein to any specific commercial product, process, or service by its trade name, trademark, manufacturer, or otherwise, does not necessarily constitute or imply its endorsement, recommendation, or favoring by the United States Government or any agency thereof, or the Regents of the University of California. The views and opinions of authors expressed herein do not necessarily state or reflect those of the United States Government or any agency thereof or the Regents of the University of California.

been determined for the first time. Surface structures were found to be projections of bulk crystal planes to the surface for both ice and naphthalene. This technique is applicable to studies of a wide variety of molecular crystal surfaces and opens the field of structural surface chemistry of organic solids to definitive investigations.

### Experimental

The experiments were performed with a standard Varian LEED apparatus, modified by the addition of a sample manipulator that could be cooled to 98K. Base pressure in the chamber was less than  $1 \times 10^{-9}$  torr. The LEED optics also served as a retarding field analyzer for Auger electron spectroscopy. A schematic diagram of the apparatus is shown in Figure 1.

The sample manipulator consisted of a bellows-sealed rotary feed-through mounted on another stainless steel bellows to allow vertical and tilt motion besides rotation of the sample. A hollow copper block  $3 \times 2 \times 1.5$  cm was attached to the shaft of the rotary feedthrough. Two 3 mm o.d. stainless steel tubes were brazed to the block for liquid nitrogen circulation. The tubes were coiled about the shaft of the manipulator (not shown in Figure 1), allowing over  $180^\circ$  rotation of the sample. The platinum crystal was spot welded to 2 platinum bars, 4 cm long, and these bars were bolted through a ceramic insulator to the copper block. Cooling of the crystal was by conduction from the copper block, and the ceramic insulator allowed simultaneous resistive heating of the crystal. The crystal could be held at any temperature between 100 and 1400 K, as measured by a chromel-alumel thermocouple spot welded to its back.

Two different Pt single crystal discs were used. They were cut from a Pt single crystal rod obtained from Materials Research Corporation, oriented to  $(111) \pm 1^\circ$ , polished and etched. A calcium impurity which segregated at the surface was removed by heating the crystal to 1700 K in  $10^{-5}$  torr of oxygen for 48 hours prior to mounting the crystal on the low temperature manipulator, and by argon ion bombardment. The crystal was cleaned of carbon before each experiment by heating it for 1/2 hour to

1200 K in  $10^{-5}$  torr of oxygen. Auger electron spectroscopy was used to demonstrate the cleanliness of the surface.

The ice and naphthalene crystal samples were produced in the vacuum chamber by allowing the respective vapors to impinge upon the cooled Pt crystal from a needle placed 1.5 cm from the crystal face. The naphthalene used was "Baker Analyzed" grade, purchased from the J. T. Baker Chemical Co. The water sample was Harleco "ultra-pure" purchased from Scientific Products Co., stated to have specific resistance of greater than  $10^7$  ohm-cm. Both were degassed before use.

The molecular flux incident upon the crystal was controlled by a leak valve. Fluxes in the range of  $10^{13}$  -  $10^{15}$  molecules  $\text{cm}^{-2} \text{sec}^{-1}$  were used. This range of fluxes was defined by the requirement of molecular flux significantly greater than the flux of chamber background gases to lessen competition during adsorption and condensation, and the requirement for convenient growth times.

The flux of molecules at the crystal surface was calibrated in two ways: optical interference, and by use of known vapor pressure versus temperature relations. The crystal could be exposed to the flux long enough to give a layer exhibiting interference colors when viewed under white light. The colors define an optical path length,<sup>5</sup> and thus a thickness that was obtained during growth in a given time. Assuming a sticking probability of the vapor molecules of unity, the molecular flux could be determined. The alternative way is to find a substrate temperature above which the molecular film would not grow. At this temperature the vaporization rate of the condensed molecules equals the rate of condensation from the vapor flux. Since the vapor pressure at this

temperature is known, the impingement rate, which must be equal, is also known. For ice,  $\log P = -\frac{2668.726}{T} + 10.43112$ <sup>6</sup>, and for naphthalene,  $\log P = -\frac{1734}{T-71} + 7.01$ <sup>7</sup> (P in torr, T in K). Neither method is extremely accurate, however the two methods yield fluxes that usually agree within a factor of 2. The heats of vaporization are 12.2 kcal/mole at 273K for ice<sup>8</sup> and 17.4 kcal/mole at 298K for naphthalene.<sup>9</sup>

ResultsIce

When water is deposited on the clean and ordered Pt(111) substrate in the temperature range of 125 - 155 K from a flux of  $10^{14}$  -  $10^{15}$  molecules  $\text{cm}^{-2} \text{sec}^{-1}$  in a thickness of  $10^1$  -  $10^4$  Å, the diffraction pattern shown in Figure 2 is obtained. The pattern consists of a hexagonal array of diffuse spots, with the spacing between them  $\sim \sqrt{3}/3$  times the spacing between the Pt(111) features. The ice pattern is rotated  $30^\circ$  from the Pt(111) pattern.

At the onset of the experiment, the Pt(111) diffraction spots are sharp, in distinct contrast to the more diffuse new spots that develop as the ice film grows. The diffraction pattern at this point could be called Pt(111)- $(\sqrt{3} \times \sqrt{3})$  R $30^\circ$ -H<sub>2</sub>O. However, as the deposition of water continues, all diffraction features become diffuse.

The diffraction pattern that can be attributed to the ordered ice crystal surface persisted as the ice film grew to a thickness of greater than 1000Å, as measured by optical interference. As the ice thickness increased, the LEED pattern deteriorated. The diffraction spots grew more diffuse, and eventually disappeared into the increasingly bright background at a thickness around 1000Å. Also, at somewhat greater thickness the ice surface charges up rapidly in the electron beam, and the space charge obliterates all of the diffraction features.

At temperatures above 155K, film growth does not take place under our conditions of vapor flux, and the Pt(111) diffraction pattern remains unchanged. At temperatures below 125K, the Pt(111) diffraction spots gradually decrease in intensity and ultimately disappear into a bright, uniform background indicating the deposition of a thick disordered ice



layer on the metal surface. Within a range of  $10^{14}$  -  $10^{15}$  molecules  $\text{cm}^{-2}$   $\text{sec}^{-1}$ , there appears to be no dependence of the quality of the diffraction pattern on incident flux. The temperature range for ordering also did not change markedly with flux.

Electron beam exposure produced little change in the diffraction pattern. Prolonged exposure (minutes, with beam current density of  $10^{-3}$   $\text{A cm}^{-2}$ ) to a thin film ( $<100 \text{ \AA}$ ) at beam energies greater than about 80 eV, can remove the ice diffraction pattern and the Pt diffraction features become visible again. Subsequent exposure of the beam damaged area to water vapor caused the ice diffraction pattern to reappear. With low beam energies (10 - 60 eV), short exposures of a thick film to the electron beam produced no noticeable change in the diffraction pattern.

#### Naphthalene

Gland and Somorjai have investigated the adsorption of naphthalene on Pt(111).<sup>10</sup> At room temperature the adsorption produced a diffraction pattern of blurred, third order features. Subsequent heating to  $150^\circ \text{C}$  produced a sharp pattern they called a (6x6). We have duplicated this work. Although the diffraction pattern of the ordered naphthalene structure may lack some of the features of a true (6x6) surface structure, for lack of a better name, this monolayer structure will be referred to as (6x6).

Slow cooling of the clean Pt(111) substrate in a flux of naphthalene vapor produced first the disordered monolayer pattern referred to above, then a diffraction pattern shown in Figure 3 consisting of concentric rings around the specular beam, with none of the Pt(111) features visible

at any voltage. Pre-cooling the substrate, then admitting naphthalene vapor produced the same diffraction pattern. Further, the same ring-like diffraction features were produced by depositing naphthalene onto a graphitic carbon covered Pt(111) surface or a clean Pt(100)-(5x1) surface.

If the Pt(111) substrate is covered with an ordered (6x6) monolayer of naphthalene, which is obtained by heating the naphthalene monolayer to 150°C for several minutes, subsequent deposition of naphthalene at temperatures 105 - 200K produced the diffraction pattern shown in Figure 4. The distances from the various order diffraction beams to the specular beam are equal to the radii of the concentric rings in the naphthalene thick layer diffraction pattern described previously. Again, the Pt(111) features were not detectable.

Both types of diffraction patterns, characteristic of azimuthally disordered and ordered growth were obtained from a thick ( $10^3$  Å) layer of naphthalene under similar conditions of temperature and incident molecular flux. With naphthalene fluxes of  $10^{14}$  -  $10^{15}$  molecules  $\text{cm}^{-2} \text{sec}^{-1}$ , thick crystals of naphthalene grew at temperatures below 200K. At temperatures below 105K neither diffraction pattern was visible, rather the pattern consisted of a uniform bright background indicating that the naphthalene deposit was disordered. Growth at temperatures approaching this lower limit of 105K produced diffraction patterns with broadened features and increased background intensity.

The diffraction patterns characteristic of well-ordered surface structures persisted as the naphthalene films grew to thicknesses greater than 1000 Å in the temperature range of 105 - 200K. At thicknesses greater than 500 Å space charge would be observed at beam voltages less

than  $\sim 30V$  -- above 30V the diffraction pattern would be clearly visible. At film thicknesses greater than 1500 Å, the presence of space charge made the LEED pattern undetectable.

The naphthalene diffraction patterns are very sensitive to electron beam exposure. In 10 seconds, at beam energies of greater than 25 eV with a beam current density of  $10^{-3} \text{ A cm}^{-2}$ , all traces of the diffraction patterns would disappear. The diffraction pattern would not again be visible from an area disordered by electron beam exposure even after subsequent deposition of naphthalene. Upon moving the beam to a fresh portion of the crystal, the pattern was again detectable. A deposited naphthalene layer could be easily evaporated by heating the crystal above 200K. If the electron beam exposure had been small, the initial naphthalene monolayer pattern, either disordered or the (6x6), was visible from the substrate after evaporation. The diffraction pattern of the substrate, after evaporation of a naphthalene layer that had been subjected to substantial electron beam exposure, showed only a faint, or no, Pt(111) diffraction features and no sign of a naphthalene monolayer pattern. The electron beam causes the naphthalene to undergo a chemical transformation (perhaps polymerization) to a disordered, more strongly bound species.

DiscussionIce

The ice diffraction pattern indicates a hexagonal surface unit mesh, 4.8 Å on a side rotated 30° from the hexagonal Pt(111) surface mesh. Within 6% this is the repeat length in a hexagonal sheet of hydrogen bonded water molecules as in the basal plane (0001) of normal hexagonal ice I, or as in the (111) plane of face centered cubic ice I<sub>c</sub>.<sup>11</sup> The structure is a network of oxygen atoms in 6-membered rings of the chair conformation with hydrogen atoms distributed between the oxygens. This structure is shown schematically in Figure 5. We conclude from the diffraction pattern that ice grows in sheets of either hexagonal (0001) or fcc (111) parallel to the Pt(111) with the two-dimensional unit cell rotated 30° to the two-dimensional Pt(111) surface unit cell. Under conditions similar to ours, the cubic form has been found to grow.<sup>12</sup> In either case the ice surface layer is not crystallographically different from a bulk lattice plane of ice, but it is that expected from the projection of a bulk ice unit cell to the hcp (0001) or fcc (111) surface. The ice crystals grow in this manner from the first monolayer outward.

Rapid (about 1 minute) cooling of the clean Pt substrate is necessary to produce ice diffraction patterns. Slow cooling allows ambient gas molecules to preferentially adsorb on the substrate before the temperature is low enough for water molecules to condense. The adsorption of gases from the ambient on the Pt(111) substrate interferes with the epitaxial growth of the ice layer. During our investigation, there was no evidence of adsorption of water on the Pt(111) surface at any temperature between 160 and 450K, in agreement with the finding of Chesters and Somorjai.<sup>13</sup>

The diffraction spot sizes are indicative of the number of scatterers in the ordered domains contributing to the spot. In the kinematic approximation, the width of the diffracted beam and the average size of the ordered domains can be related by the Scherrer equation<sup>14</sup>

$$\Delta = \frac{\lambda}{L \cos\theta}$$

where  $\Delta$  is the angular line width of the spot,  $\lambda$  the wavelength of the electron,  $\theta$  the diffraction angle and  $L$  the domain width. This equation gives 40 Å for the size of the ordered domains of the growing ice film. For the thickest layers, the domain size is reduced below 30 Å. The 6% lattice mismatch between the ice crystal lattice and the Pt(111) surface perhaps contributes to this limited domain size by introducing dislocations into the ice to reduce lattice strain.

The deposition of a disordered phase of ice at temperatures below 110K has been reported during X-ray and electron diffraction studies.<sup>12</sup> the disordered phase was reported to crystallize as the temperature was raised, which has not been observed in this study.

The ice film shows little damage under exposure by the electron beam. High energy beams and long exposure evaporate ice from the growing film, allowing Pt diffraction features to be seen. The production of ionized clusters of water molecules from a film of condensed water vapor by an 80 eV electron beam has been reported<sup>15</sup> and this process is probably also occurring during our experiments. If the beam is not allowed to penetrate the entire ice film, electron beam exposure produces no change in the pattern. The electron energies are high enough to chemically alter the ice surface or to disorder the surface by rearranging the water molecules but neither of these processes are evident.

The ice crystal, an insulator, does not charge up until thicknesses of well over 1000 Å, allowing LEED experiments to be performed on samples of less than this thickness. Hamill<sup>16</sup> also observed ice films of several hundred angstrom thickness did not charge up under an electron beam. The mechanism of the removal of charge is not clear, however Matskevich and Mikhailova report a secondary electron emission coefficient for ice of 2.2 at 100 eV.<sup>17</sup> If the secondary electron emission coefficient remains that high at the lower voltages used for our observations, negative surface charge would be easily removed.

#### Naphthalene

From the diffraction patterns of the naphthalene crystals, a well-defined naphthalene surface structure may be deduced. This can be identified as the ab plane (001) of the bulk naphthalene crystal. Figure 6 shows the arrangement of naphthalene molecules in this place. The unit cell derived from the diffraction pattern is within 1% of the reported bulk X-ray unit cell projection distances. These are  $|\vec{a}| = 8.235 \text{ Å}$  and  $|\vec{b}| = 6.003 \text{ Å}$ .<sup>18</sup> The ring-like diffraction pattern that appears upon growth of the naphthalene crystals on the clean Pt(111) or on a disordered monolayer indicated the ab plane grows parallel to the Pt(111) but there is no preferred azimuthal orientation. In the growth of naphthalene on the Pt(111)-(6x6) naphthalene structure which produced discrete diffraction spots, the naphthalene crystals again grow with the ab parallel to the Pt(111), but the a ([100]) of each crystallite is always parallel to one of the interatomic directions in the platinum surface. The observed weakness of the (h, k) features where h + k is odd is consistent with the presence of two orientationally inequivalent naphthalene molecules lying in

the ab crystal plane. The surface structure of the solid naphthalene appears to be no different from a lattice plane ((001)) of the bulk crystal.

It is evident that the structure that shows the (6x6) pattern orients the subsequent thick layer naphthalene growth. The best lattice matching between the Pt(111) and the naphthalene crystal structure occurs when the a of the naphthalene lies parallel to the interatomic directions of the Pt (Pt-Pt = 2.77 Å,  $|\vec{a}| = 8.235 \text{ Å}$ ,  $3(2.77) = 8.3 \text{ Å}$ ). Yet this orientation only occurs upon the (6x6) monolayer structure. The precise location of the naphthalene molecules in the (6x6) surface structure awaits structure analysis using the diffraction beam intensities.

Diffraction spot sizes in naphthalene indicate domain sizes of 70 Å over the range of thickness observed. These are somewhat larger domains than found in the ice growth. The closer registry with Pt lattice (1% compared to 6% for ice) may contribute to better ordering. The hexagonal symmetry of the diffraction pattern and the limited domain size suggest that the naphthalene film consists of a large number of crystallites with the ab plane parallel to the Pt surface, oriented in six equivalent directions. Grain boundaries separate the crystallites.

The electron beam has a marked destructive effect on the naphthalene crystals. The naphthalene is transformed into a different chemical species of lower vapor pressure that does not desorb from the Pt(111) at temperatures less than 100°C. The deposit, perhaps a polymer, interferes with subsequent naphthalene growth, so that no diffraction pattern is visible from the damaged area even after attempts to regrow the naphthalene crystal on top of the damaged area.

Similar decomposition of condensed benzene by low-energy electron bombardment has been reported.<sup>19</sup> This behavior is in contrast to the stability of the naphthalene (6x6) monolayer pattern which was found to resist electron beam damage. Research on electron stimulated desorption showed that electron induced dissociation and desorption cross sections are orders of magnitude lower for chemisorbed molecules than for free molecules and lower for chemisorbed molecules than for physically adsorbed molecules. De-excitation of the molecule through the metal before decomposition can occur is believed to be the explanation.<sup>20</sup> The same argument may be used to explain the electron beam sensitivity of the naphthalene crystal surface in comparison to the chemisorbed monolayer of naphthalene on platinum. There is no rapid recombination path to the ground state for an electronically excited naphthalene molecule as it is only weakly interacting with the neighboring molecules in the crystal.

As in the case of ice, the naphthalene films also do not trap excess charge if the films are thin enough. For films of intermediate thickness ( $\sim 500$  Å) charging below a certain beam voltage and not above it again suggests secondary electron emission as a mechanism of charge removal.

#### Ice and Naphthalene

The two crystal faces found to grow from two dissimilar molecules in this study exhibit two similarities. 1) They are both closely packed faces of the lowest surface free energy. The naphthalene ab is the closest packed plane in the naphthalene crystal. The ice I and ice I<sub>C</sub> structures are open structures, as dictated by the intermolecular hydrogen bonding, but the hexagonal sheet of water molecules observed is the closest packed



plane in these structures. 2) They both exhibit lattice constants closely related to the Pt(111) lattice constants. In terms of the Pt-Pt distance  $d = 2.77 \text{ \AA}$ , the ice surface lattice constant is within 6% of  $\sqrt{3} d$  and both the Pt(111) and the ice surface are hexagonal. The  $\vec{a}$  length in naphthalene is within 1% of  $3 d$  and the  $\vec{b}$  length is within 1% of  $2 \frac{1}{2} \times \sqrt{3}/2 d$ , the repeat distance in the  $\underline{b}$  direction being  $\sqrt{3}/2 d$ . These two properties may have determined the selection of which plane grows parallel to the substrate. In future studies we shall explore the importance of matching the lattice parameters or the strength of the interaction of the molecule-metal monolayer by using other metal substrates of the same orientation. Preliminary results of naphthalene growth on Pt(100) gave no azimuthal orientation of the crystals, thus rotational symmetry of the substrate is important in inducing ordering.

The two materials also behaved similarly in the dependence of film quality on substrate surface preparation. Naphthalene grew with azimuthal orientation on the Pt(111)-(6x6) naphthalene, and without azimuthal orientation on a disordered monolayer. Ice would show good crystallinity and orientation when grown on clean Pt(111) and either no crystallinity or poor orientation on a poorly prepared surface. These results have implication for the processes of vapor phase epitaxy.

Summary

Low-energy electron diffraction patterns have been observed from two molecular crystal surfaces, the ice I (0001) or ice I<sub>c</sub> (111) and the naphthalene ab (or (001)). The surface structures of these molecular crystals appear to be identical to projection of lattice planes of the known bulk crystal structures. The molecular crystals were grown epitaxially on the Pt(111) surface and the LEED patterns are detectable without interference from surface space charge when the crystals are less than  $10^3$  Å thick. The growth of ice and naphthalene upon Pt(111) from the vapor phase at low pressures and temperatures is dependent on the structure of the platinum surface. Identical growth conditions can yield ordered, rotationally disordered or completely disordered surfaces of the molecular crystals, as observed by LEED, depending on the cleanliness and order of the Pt surface.

The electron beam probe damages the surfaces of molecular crystals but LEED studies can be carried out successfully. To minimize decomposition or desorption of the surface layers of molecular crystals, the electron beam exposure should be minimized.

Acknowledgement

This work was supported by the U. S. Energy Research and Development Administration.

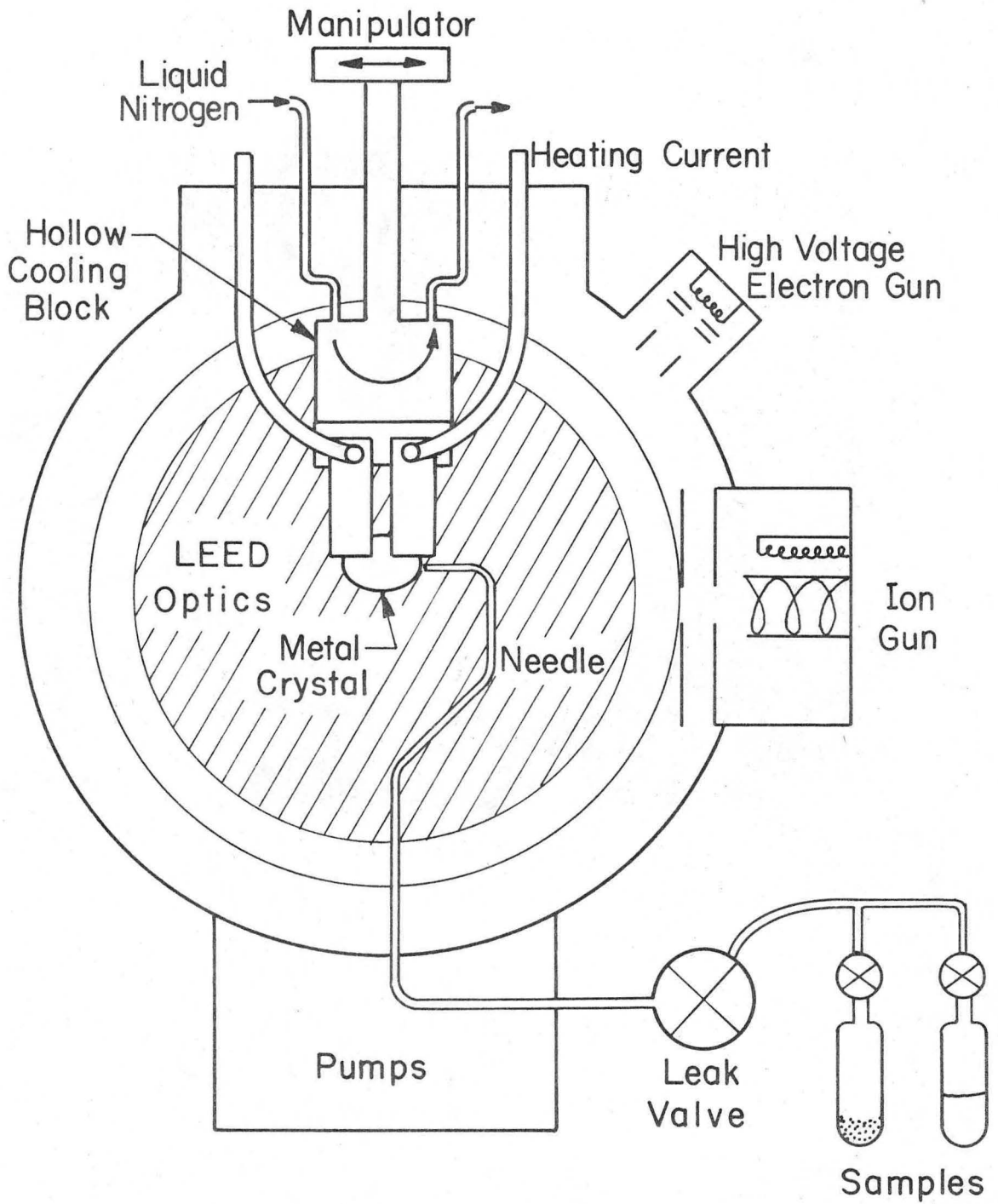
References

1. L. E. Firment and G. A. Somorjai, J. Chem. Phys. 63, 1037 (1975).
2. H. H. Farrell, M. Strongin and J. M. Dickey, Phys. Rev. B 6, 4703 (1972).
3. A. Ignatiev and T. N. Rhodin, Phys. Rev. B 8, 893 (1973).
4. A. Ignatiev, T. N. Rhodin and S. Y. Tong, Surface Sci. 42, 37 (1974).
5. Michael L. Sand, M. S. Thesis, University of California, Berkeley.
6. G. Jancso, J. Pupezin and W. A. Van Hook, J. Phys. Chem. 74, 2984 (1970).
7. B. J. Zwolinski and R. C. Wilhoit, Handbook of Vapor Pressures and Heats of Vaporization of Hydrocarbons and Related Compounds. American Petroleum Institute Project 44 and Thermodynamics Research Center Publication No. 101, College Station, Texas, (1971) 71.
8. D. Eisenberg and W. Kauzmann, The Structure and Properties of Water. (Oxford Univ. Press, London, 1969) 100.
9. B. J. Zwolinski and R. C. Wilhoit, op. cit., 289.
10. J. L. Gland and G. A. Somorjai, Surface Sci. 38, 157 (1973).
11. D. Eisenberg and W. Kauzmann, op. cit., 71.
12. Ibid., 89-91.
13. M. A. Chesters and G. A. Somorjai, Surface Sci. (To be published).
14. A. Guinier, X-ray Diffraction. (W. H. Freeman and Co., San Francisco and London, 1963) 121.
15. G. R. Floyd and R. H. Prince, Nature Physical Sci. 240, 11 (1972).
16. L. M. Hunter, D. Lewis and W. H. Hamill, J. Chem. Phys. 52, 1733 (1970).
17. T. L. Matskevich and E. G. Mikhailova, Fiz. Tverd. Tela. 2, 709

- (1960) [Sov. Phys. Solid State 2, 655 (1960)].
18. R. W. G. Wyckoff, Crystal Structures. (Interscience, New York 1963) Vol. 6, pt. 2, 383.
  19. K. Hiroaka and W. H. Hamill, J. Chem. Phys. 57, 3870 (1972).
  20. T. E. Madey and J. T. Yates, Jr., J. Vac. Sci. Tech. 8, 525 (1971).

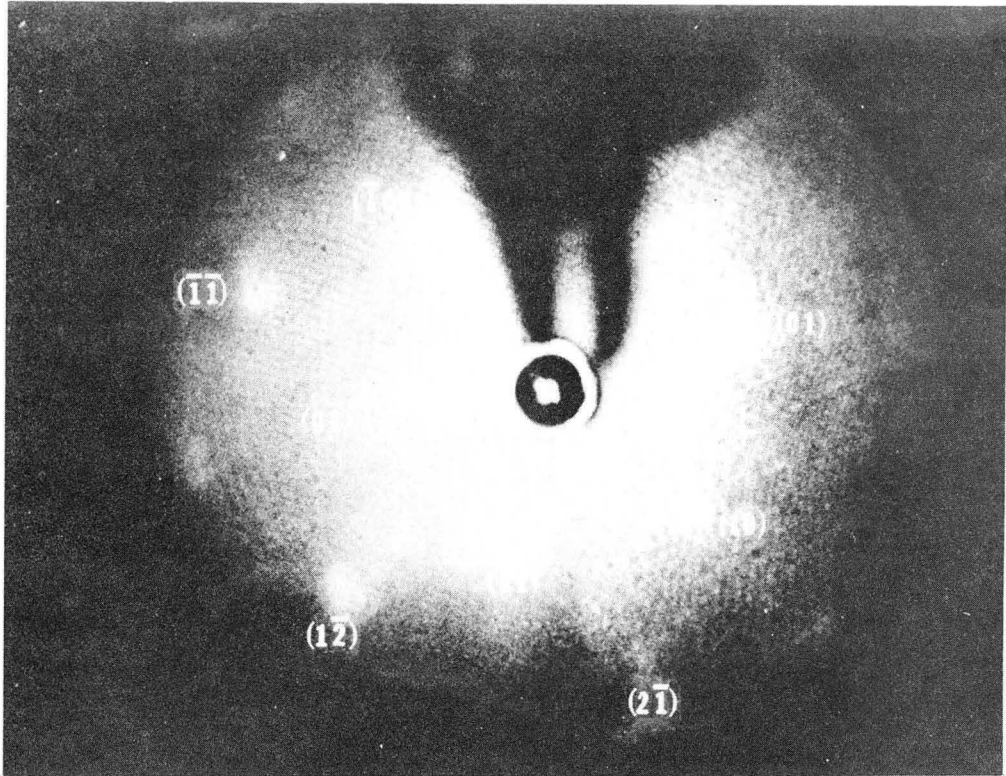
Figure Captions

1. Schematic of experimental chamber.
2. LEED pattern of the ice surface at 74 eV.
3. (a) LEED pattern at 14.4 eV of a naphthalene crystalline film prepared by deposition onto a disordered monolayer on Pt(111). (b) Diagram of (a) with several rectangular unit cells of the reciprocal lattice shown. This unit cell, present in all azimuthal orientations, reproduces the diffraction pattern. Rings from spots  $(\underline{h}, \underline{k})$  with  $\underline{h} + \underline{k}$  odd are dim (see text).
4. (a) LEED pattern at 36.5 eV of naphthalene crystalline film prepared by deposition onto an ordered naphthalene monolayer on Pt(111). (b) Diagram of (a) with three orientations of the reciprocal unit cell indicated. Spots due to the three types of domains are shown by different symbols: circles, squares, or triangles. As in Figure 3, spots with  $\underline{h} + \underline{k}$  odd are dim.
5. Proposed surface structure of ice. The ice surface mesh is indicated by light lines, the Pt(111) surface unit cell is drawn with correct orientation at lower left. The oxygen atoms of the water molecules are indicated by circles with the open circles lying above the plane of the filled circles. Dimensions shown for the ice lattice are bulk ice values.<sup>9</sup>
6. Proposed surface structure of naphthalene ab plane with the Pt(111) surface unit cell drawn with correct orientation at lower left. Magnitudes of a and b vectors shown are those for bulk naphthalene.<sup>17</sup>



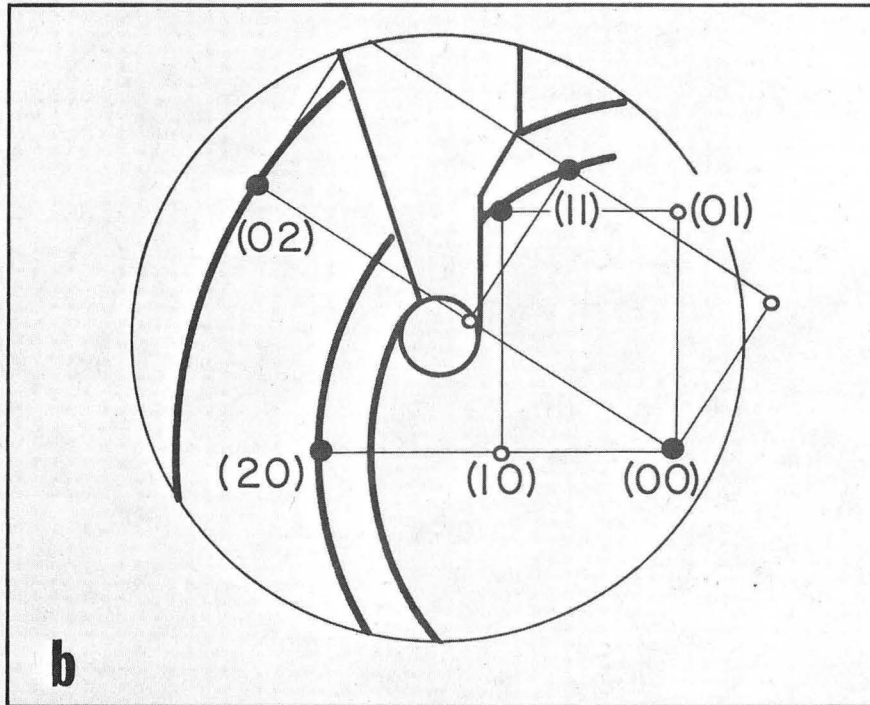
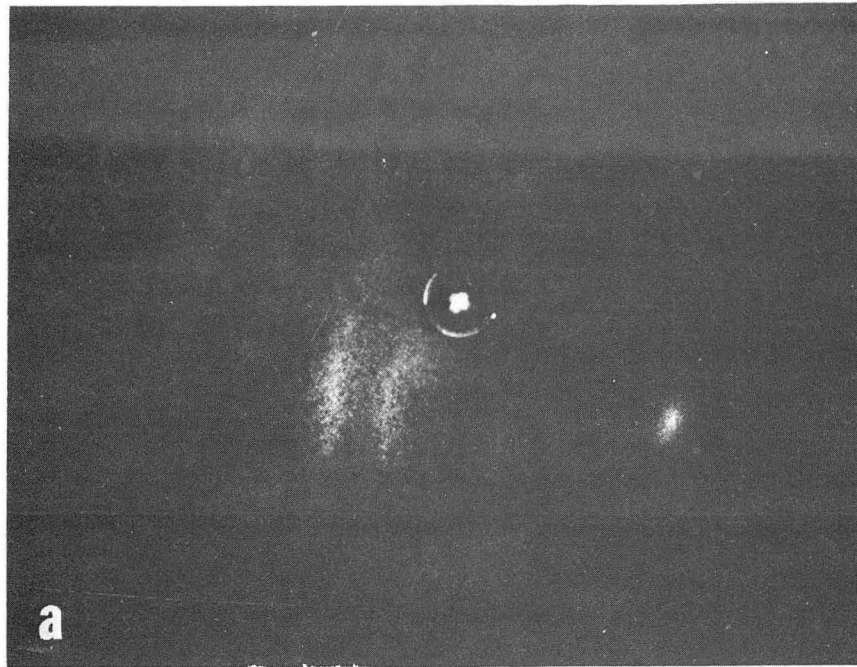
XBL 757- 6645

Fig. 1



XBB 7510-7375

Fig. 2

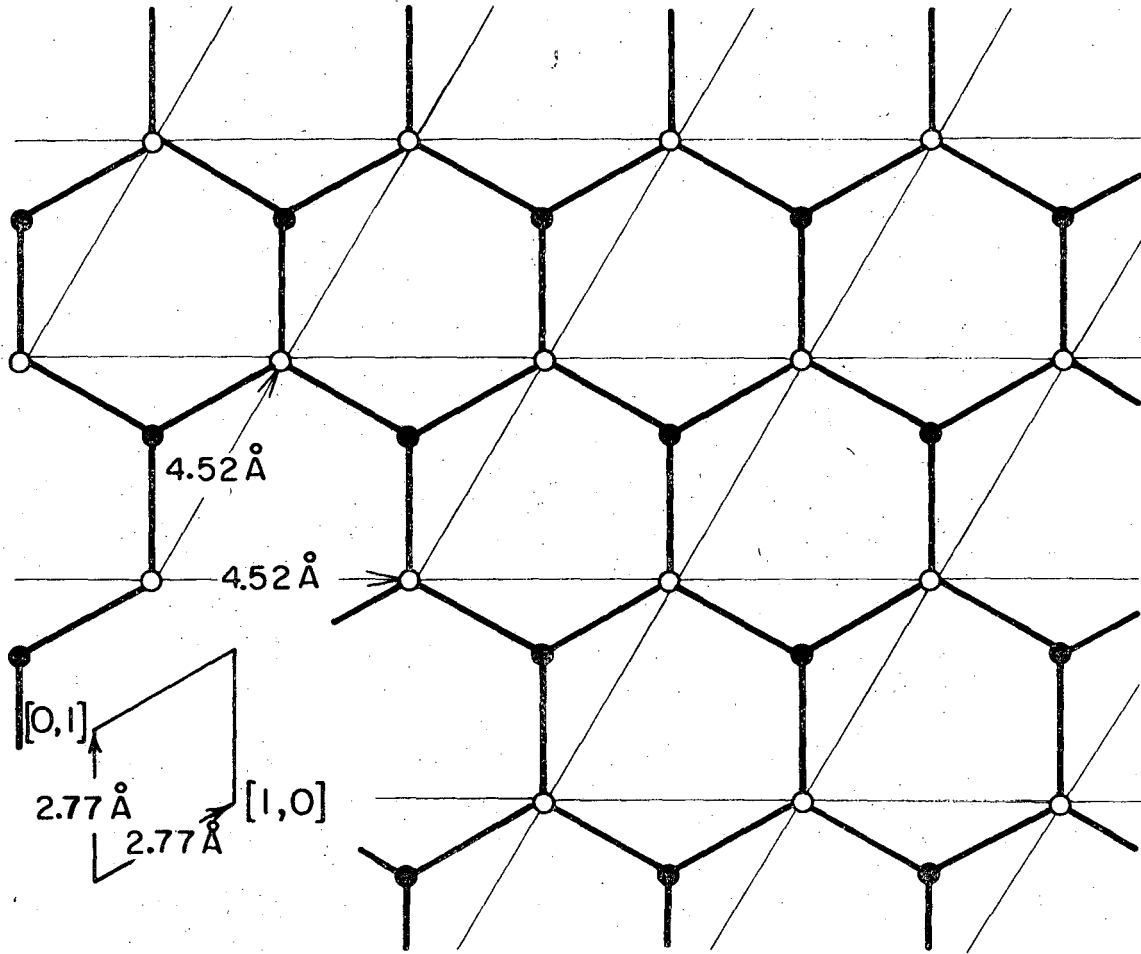


XBB 757-5041

Fig. 3

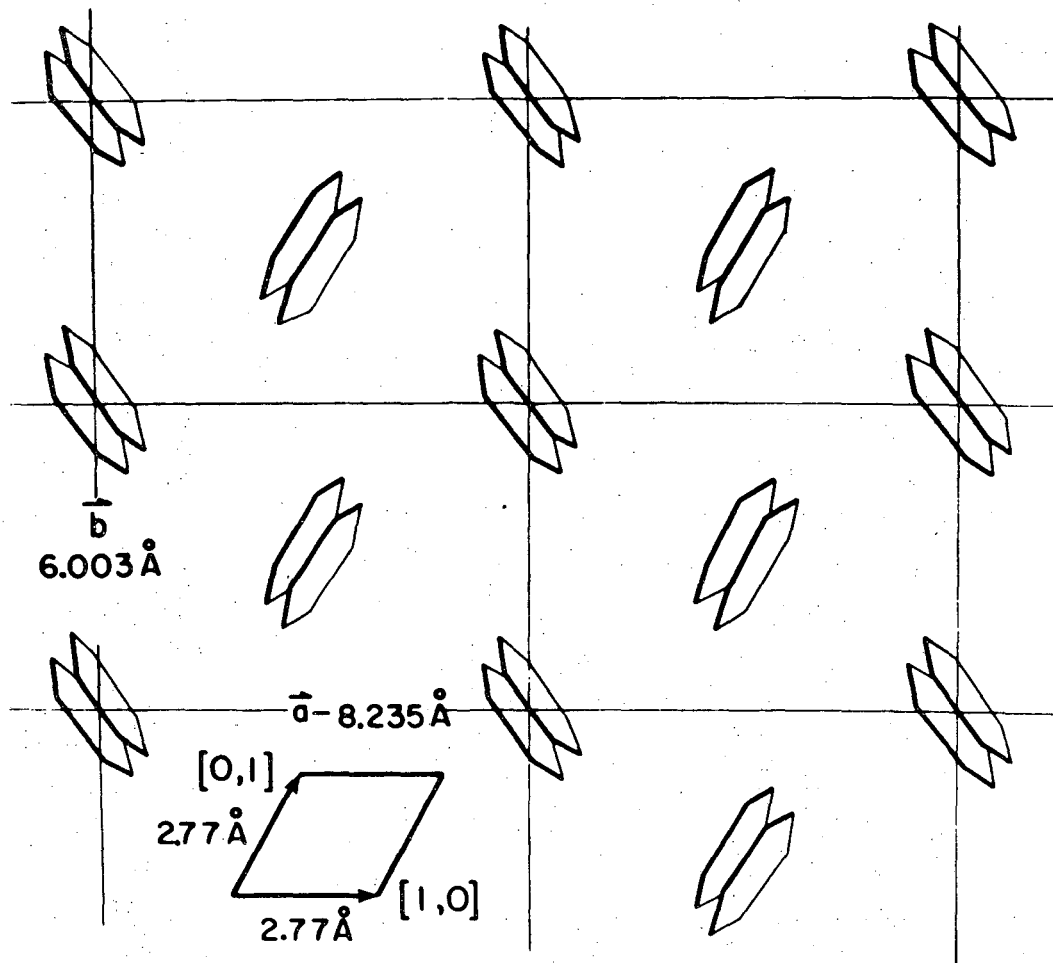






XBL7412-8376

Fig. 5



XBL 7510-7402

Fig. 6

**LEGAL NOTICE**

*This report was prepared as an account of work sponsored by the United States Government. Neither the United States nor the United States Energy Research and Development Administration, nor any of their employees, nor any of their contractors, subcontractors, or their employees, makes any warranty, express or implied, or assumes any legal liability or responsibility for the accuracy, completeness or usefulness of any information, apparatus, product or process disclosed, or represents that its use would not infringe privately owned rights.*

TECHNICAL INFORMATION DIVISION  
LAWRENCE BERKELEY LABORATORY  
UNIVERSITY OF CALIFORNIA  
BERKELEY, CALIFORNIA 94720